Rare Metal Materials and Engineering
Volume 52, Issue 2, February 2023
Available online at www.rmme.ac.cn

Science Press

Cite this article as: Wang Wensi, Liu Hui, Yu Zejin, et al. Golf-like (V, Ru)-co-doped NiS_2 Microspheres as Efficient Electrocatalysts for Hydrogen Evolution Reaction in Alkaline Media[J]. Rare Metal Materials and Engineering, 2023, 52(02): 461-469.

ARTICLE

Golf-like (V, Ru) -co-doped NiS_2 Microspheres as Efficient Electrocatalysts for Hydrogen Evolution Reaction in Alkaline Media

Wang Wensi[1], Liu Hui[1], Yu Zejin[1], Lu Jun[3], Feng Feng[1], Huan Yuanfeng[1], Zhao Yunkun[1], Yu Jianmin[3], Qing Shan[2], Bi Xiangguang[1,2]

[1] Kunming Sino-Platinum Metals Catalyst Co., Ltd, Kunming 650106, China; [2] Faculty of Metallurgical and Energy Engineering, Kunming University of Science and Technology, Kunming 650106, China; [3] Kunming Institute of Precious Metals, Kunming 650106, China

Abstract: Vanadium and ruthenium were introduced into NiS_2 via solvothermal method and ruthenium drop method (room temperature) to prepare (V, Ru)-co-doped NiS_2 microspheres coated on Ni foam ((V, Ru)-NiS_2/NF) as electrocatalysts. The rough golf-like structure allowed the exposure of abundant active sites via sulfuration process. Moreover, the cooperation of vanadium and ruthenium could optimize the electronic structure of NiS_2, provide extra catalytically active sites, and further strengthen the intrinsic catalytic activity. Besides, the addition of nickel foam could support the catalytic material, avoid the aggregation, and enhance the conductivity. Results show that the obtained (V, Ru) -NiS_2/NF electrocatalysts exhibit excellent electrocatalytic performance and superior stability for hydrogen evolution reaction (HER) in alkaline media. At the current density of 10 $mA \cdot cm^{-2}$, the presented (V, Ru)-NiS_2/NF delivers an overpotential of 38 mV, which is smaller than that of commercial Pt/C, and possesses lower Tafel slope (80.3 $mV \cdot dec^{-1}$), higher relative electrochemical active surface area (ECSA) and excellent durability in 1 mol/L KOH for 24 h.

Key words: vanadium; ruthenium; doping; hydrogen evolution reaction

With the development of global economy and the increasing demand for natural resource, hydrogen (H_2) fuel as a new chemical energy gradually replaces fossil fuels over time because of its zero-carbon emission, abundant resources and high-energy density[1–5]. There are many approaches to generate hydrogen, for example, photocatalytic[6–8], electrocatalytic[9–12]. Taking into account all aspects of technology and cost, hydrogen evolution reaction (HER) technology is one of the promising methods to generate H_2, which has attracted considerable attention from all over the world. Currently, precious metal materials (Pt, Pd, Rh, etc) show excellent HER performance, and they can maintain the lower overpotential and higher current density, but they have problems such as poor stability and high cost in large-scale industrialization[13–16]. Hence it is imperative to find an efficient and environmentally friendly electrocatalyst to replace precious metal materials for HER. Due to their low cost, low toxicity and abundant reserves, sulfides are regarded as the most promising candidates[17–18]. In spite of this, the HER activity of the sulfide catalysts is inferior to that of precious metal catalysts. Therefore, researchers have adopted a variety of strategies to enhance the HER activity of transition metal sulfide electrocatalyst, such as morphology designing, high-index facts, element doping, lattice strains and defect engineering[19–22].

In particular, NiS_2, which has large active area and high conductivity, is recognized as one of the most excellent HER electrocatalysts and has been widely reported in recent years[23–25]. Kuang et al[26] firstly designed and prepared a novel sandwich-like architecture NiS_2/V-MXene HER electrocatalyst which showed lower overpotential and stable durability, and DFT results proved that there is a strong electronic

Received date: May 06, 2022
Foundation item: Platinum Group Metal Environmental Treatment and Key Technology Research and Application Demonstration of New Chemical Catalytic Materials (202102AB080007)
Corresponding author: Bi Xiangguang, Ph. D., Senior Engineer, Kunming Sino-Platinum Metals Catalyst Co., Ltd, Kunming 650106, P. R. China, E-mail: xiangguang.bi@spmcatalyst.com

interaction between NiS_2 and V-MXene, indicating that NiS_2 can provide faster electronic transfer rate and more catalytic sites for V-MXene material, and play an important role in improving electrocatalytic activity. Li's group[27] developed a novel NiS/NiS_2 hetero-material which had an amorphous interface via the one-step thermal decomposition method. The NiS/NiS_2 interwoven heterostructure prepared by inducing phase change possesses more active sites and faster electron transfer rate and can further reduce charge-transfer resistance and Gibbs free energy. Finally, the synthesized NiS/NiS_2 electrocatalyst displays outstanding electrocatalytic performance and durability for HER, OER (oxygen evolution reaction) and OWS (overall water splitting). Moreover, Kuang's group[28] synthesized three-dimensional (3D) hollow structure MoS_2-NiS_2 nanoparticles coated on nitrogen-doped graphene foam (NGF) via hydrothermal and CVD methods. Benefiting from the heterogeneous interface between MoS_2-NiS_2 and NGF, the MoS_2-NiS_2/NGF electrocatalyst which processed more active sites and faster electron transfer rate, exhibited superior HER, OER and OWS performance than MoS_2/NGF and NiS_2/NGF. However, in the current reports, the catalytic performance of NiS_2 is far less than that of Pt-based catalysts, which inspired us to redesign and to prepare new NiS_2-based electrocatalysts.

Up to date, element doping is always the most efficient method to improve HER activity, such as Fe[29], Co[30], Ni[31], V[32]. Introducing metal ion can enhance the conductivity of catalyst and adjust the electronic structure, thus improving the intrinsic activity. Wang et al[33] designed and prepared V-doped Ni_3S_2/Ni_xP_y nanosheets, which showed excellent HER performance with lower overpotential and good stability. The reason for the outstanding HER activity is that V doping can enhance the conductivity of Ni_3S_2/Ni_xP_y, and then accelerate the electron transfer rate. Furthermore Yan[34] introduced Fe (III) into the lattice of the NiS_2 (002), and synthesized a new and high-efficiency Fe-NiS_2 electrocatalyst with a lower Tafel slope of 37 $mV \cdot dec^{-1}$ and a smaller overpotential of 121 mV at 10 $mA \cdot cm^{-2}$. The DFT results proved that such excellent photocatalytic and electrocatalytic properties are due to the fact that the incorporation of Fe (III) reduces the energy barrier for hydrogen production. At the same time, noble metals with high activity were also used as dopants for the hydrogen evolution reaction, for example, a unique and novel ganoderma-like MoS_2/NiS_2 electrocatalyst with high-loading Pt atoms was firstly designed and developed by Guan and co-workers[35], which showed superior catalytic activity and excellent durability for 72 h. Therefore, metal doping is regarded as an effective approach to enhance the electrocatalytic activity. Ruthenium, one of the cheapest precious metals, has electrocatalytic activity similar to Pt. Most of the research reported that ruthenium compounds are prepared to ruthenium phosphide at low temperature for hydrogen evolution reaction[36–38], but there are few reports on ruthenium used as doping agent to enhance the activity.

Considering the above two aspects, we researched golf-like (V, Ru)-co-doped NiS_2 coated on conductive nickel foam ((V, Ru)-NiS_2/NF) as a high-efficiency and low-cost HER electrocatalyst in 1 mol/L KOH through solvothermal method and vulcanization at low temperature. The unique golf-like structure had rough surface and larger contact area, which could accelerate contact with electrolytes and speed up the HER reaction. Moreover, the nickel foam could better disperse the material and avoid aggregation affecting the catalytic activity. The introduction of vanadium and ruthenium could not only optimize the electronic structure of NiS_2 and enhance its electrical conductivity, but also acted as additional active sites for HER. The obtained (V, Ru)-NiS_2/NF composite exhibited superior catalytic performance in alkaline solution with an overpotential of 38 mV at 10 $mA \cdot cm^{-2}$, a low Tafel slope of 80.3 $mV \cdot dec^{-1}$ and an excellent stability for 24 h.

1 Experiment

1.1 Preparation of Ni-V hydroxide/NF

First, 0.5 mmol $Na_3VO_4 \cdot 12H_2O$, 1 mmol $NiCl_2 \cdot 6H_2O$, 5 mmol urea and 6 mmol NH_4F were added to 30 mL deionized water. After complete dissolution, the solution was added to a reactor containing 1 cm×4 cm nickel foam. The autoclave was placed in a heating oven, heated to 160 °C for 16 h, and after the Teflon-lined stainless autoclave was cooled to room temperature, yellow nickel foam was obtained, rinsed three times with ethanol and deionized water, and placed in a vacuum drying oven to dry.

1.2 Preparation of Ru-NiV hydroxide/NF

First, 25 mg of Ru (III) 2, 4-pentanedionate was weighed, then dissolved in 1 mL of ethanol, ultrasonically form a dispersion solution, and the prepared solution was dropped on NiVOH/NF and finally dried at room temperature. Then the red Ru-NiV hydroxide/NF was obtained.

1.3 Preparation of V, Ru-NiS_2/NF

The red Ru-NiV hydroxide/NF placed in a 1 cm×6 cm porcelain boat was placed in the center of the tube furnace, and a porcelain boat with 0.5 g sulfur powder was placed at upstream of the tube furnace. The reaction system was heated to 350 ° C and maintained for 2 h, and the tube furnace chamber was cooled down naturally. In contrast, $Ni(OH)_2$/NF and V-NiS_2/NF took the same steps for synthesis.

1.4 Electrochemical measurements

The crystal structures of the samples were examined by powder X-ray diffraction (XRD, Bruker D8 Advance). The morphology of the catalysts coated on Ni Foam was characterized by SEM (FEI quanta FEG 250). The elemental valence of different samples located on surface was analyzed by multifunctional imaging electron spectrometer (Thermo ESCALAB 250Xi). The morphology of the (V, Ru)-NiS_2/NF was further characterized by TEM (JEOL JEM-2100F) and TEM image was recorded by Oxford IncaEnergy X-max 80T.

1.5 Characterization

The HER performance was examined by a Gamry (reference 3000) workstation at room temperature in alkaline solution. Through a three-electrode system, the catalysts supported on Ni foam were used as the working electrode, and

the calomel electrode and the graphite rod were used as the reference and counter electrodes, respectively. Typically, the linear sweep voltammetry (LSV) curve was measured at a scan rate of 2 $mV \cdot s^{-1}$. The electrochemical impedance spectroscopy (EIS) test was conducted at the frequency ranging from 100 kHz to 0.01 Hz with an overpotential of 150 mV in alkaline solutions. In addition, the time-dependent current density was tested for 24 h to prove its stability.

2 Results and Discussion

Through X-ray diffraction (XRD), the crystal structures of as-prepared samples were investigated. As displayed in Fig. 1, there are five diffraction peaks located at 22.7°, 33.4°, 34.4°, 38.7° and 59.9°, which correspond to the standard card of the α-$Ni(OH)_2$ (PDF # 38-0715) and demonstrate that the green powder on the surface of nickel foam is $Ni(OH)_2$. Apart from this, three strong diffraction peaks of 44.5°, 51.8° and 76.3° are indexed to the standard card of the Ni (PDF # 04-0850). And then we added vanadium source to the sample, as shown in Fig.2, the diffraction peaks at 22.7°, 33.4°, 34.4°, 38.7° and 59.9° also match well with the standard card of the α-$Ni(OH)_2$, indicating that when adding vanadium source to the composite, the crystal structure of as-synthesized samples will not change, indicating that vanadium have no influence on the crystal structure. After sulfuration at low temperature, except for the diffraction peaks of nickel foam, some diffraction peaks appear at 31.4°, 35.2°, 38.7°, 45.0°, 53.3°, 58.4°, 60.9° in Fig. 3a, which correspond to the standard card of the NiS_2 (PDF # 89-1742). There are no other diffraction peaks about vanadium and ruthenium, indicating that the content of vanadium and ruthenium compound on the surface is too low to be detected[39].

The morphology of $Ni(OH)_2$/NF, Ni-V hydroxide/NF and (V, Ru)-NiS_2/NF was investigated by SEM and TEM. Fig. 4 exhibits the images of $Ni(OH)_2$/NF products. The $Ni(OH)_2$/NF precursor is composed of many sheets with size of 3–4 μm and a thickness of tens of nanometers. The nanosheets are uniformly distributed on the nickel foam and the surface is

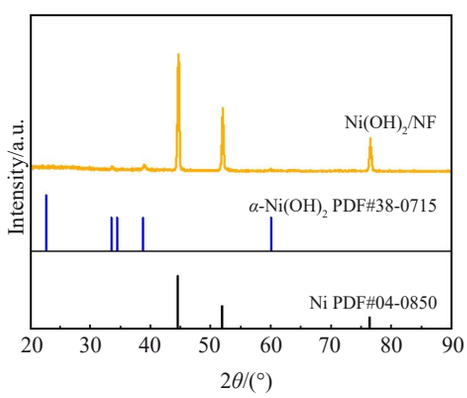

Fig.1 XRD patterns of Ni hydroxide/NF

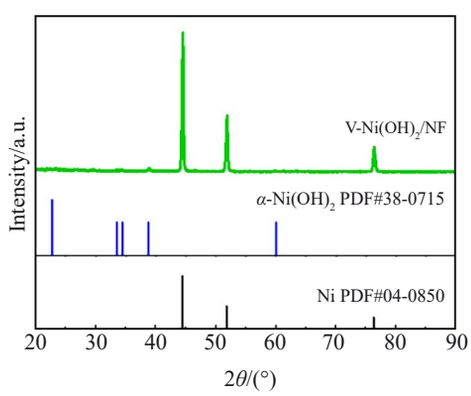

Fig.2 XRD patterns of Ni-V hydroxide/NF

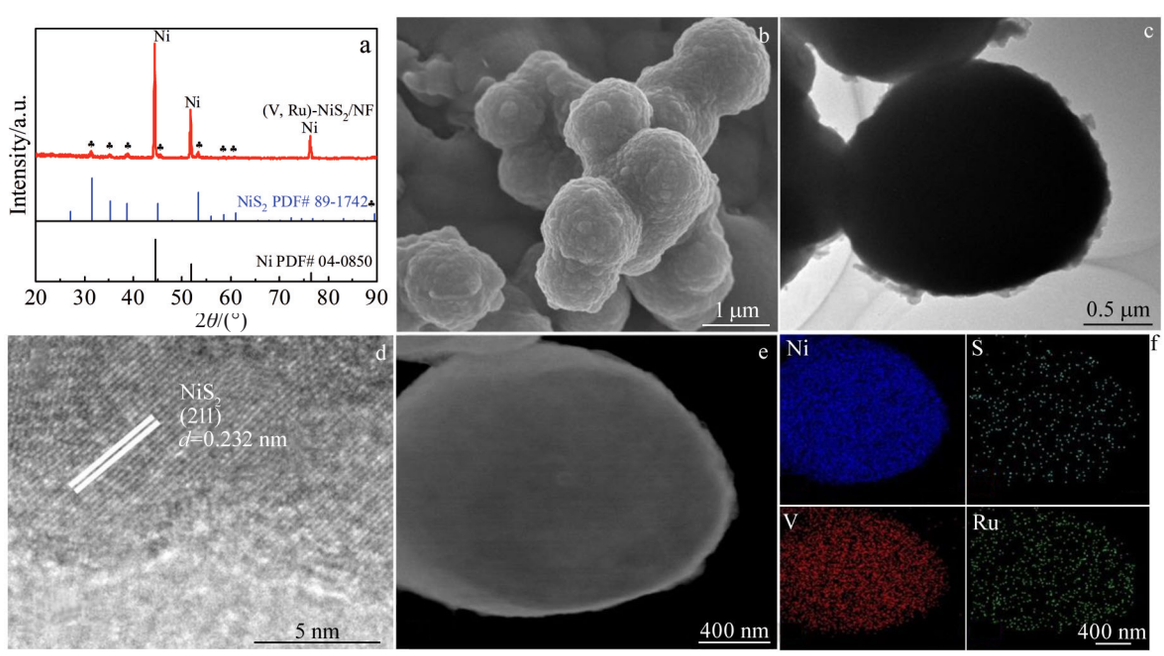

Fig.3 XRD patterns (a), SEM images (b, e), TEM image (c), HRTEM image (d) and corresponding EDS mappings (f) of (V, Ru)-NiS_2/NF

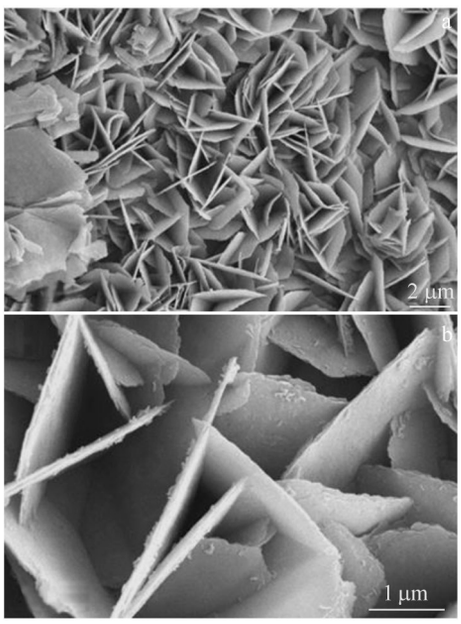

Fig.4 SEM images of Ni hydroxide/NF

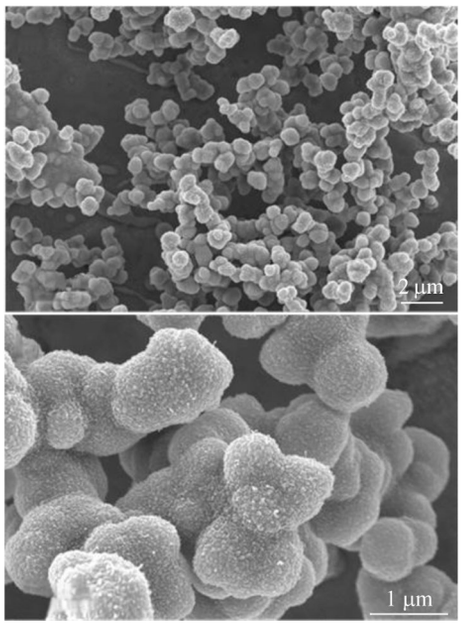

Fig.6 SEM images of V-NiS_2/NF

smooth without obvious impurities. When $Na_3VO_4 \cdot 12H_2O$ is added into the reaction system, the morphology of as-prepared sample is characterized. It is found that the morphology changes greatly and it is composed of many uniform spheres with a size of 3 μm in Fig.5, demonstrating that vanadium has a great influence on the morphology of the samples. After vulcanization of the above precursor, Fig. 6 exhibits that V-NiS_2/NF is composed of many irregular micron particles. After sulfuration treatment, SEM image (Fig. 3b) of (V, Ru)-NiS_2/NF shows that many golf-like spheres are closely connected with a size of approximately 2 μm and grow on the surface of NF. The surface of the as-synthesized samples is greatly rough, which is beneficial to increase active area and to accelerate the diffusion of electrolytes. As displayed in Fig. 3c, transmission electron microscopy can directly visualize the morphology and structure of the product. The TEM images of (V, Ru)-NiS_2/NF display similar golf-like spheres morphology with a diameter of 2 μm, which is in accordance with SEM results. From HRTEM results in Fig. 3d, the microspheres display the lattice spacing of 0.232 nm, which can be distributed to the (211) plane of NiS_2. To verify the element distribution of the as-prepared samples, the EDS mapping is adopted. As shown in Fig. 3e, the mappings confirm the existence of Ni, S, V and Ru elements which are evenly distributed, and prove that V and Ru elements are successfully doped into NiS_2.

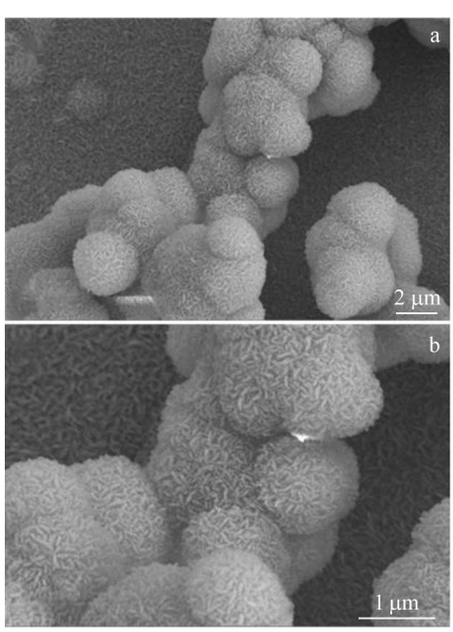

Fig.5 SEM images of Ni-V hydroxide/NF

At the same time, we also used X-ray photoelectron spectroscopy (XPS) technology to analyze the elemental valence and substance composition of (V, Ru)-NiS_2/NF and Ni-V hydroxide/NF. Fig. 7a and Fig. 7b shows the XPS spectra of Ni 2p and V 2p. The diffraction peaks at 855.7 and 874.1 eV can be attributed to Ni $2p_{3/2}$ and Ni $2p_{1/2}$, respectively, while the diffraction peaks at 861.4 and 880.3 eV next to the main peak mainly correspond to satellite peaks of Ni element. However, the diffraction peak of nickel foam is mainly located at 853.3 and 872.0 eV. For the precursor Ni-V hydroxide/NF, the diffraction peaks at 856.8 and 874.4 eV mainly correspond to Ni $2p_{3/2}$ and Ni $2p_{1/2}$, respectively as shown in Fig. 8a. After sulfuration treatment, the diffraction peaks of Ni 2p of (V, Ru)-NiS_2/NF have a negative shift compared with that of Ni-V hydroxide/NF. The S 2p spectrum is shown in Fig. 8b. The peaks located at 162.7 eV can be assigned to S $2p_{3/2}$ and the peak located at 163.8 eV belongs to S $2p_{1/2}$, which indirectly proves the existence of metal-S bond in the compound, indicating that the sample is successfully vulcanized. Moreover, the satellite peaks at 162.5 and 165.2 eV are mainly

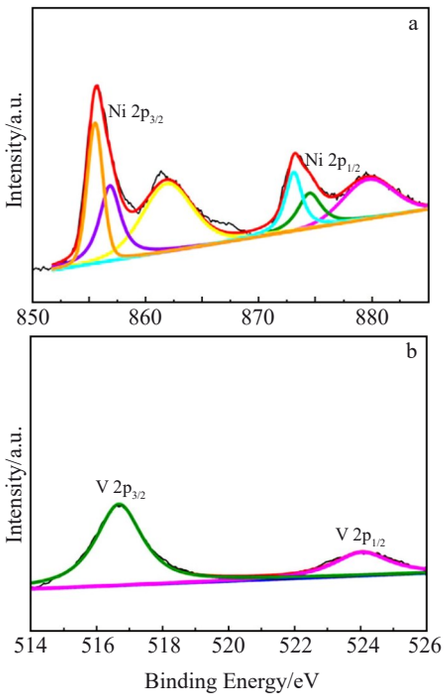

Fig.7 XPS spectra of Ni-V hydroxide/NF: (a) Ni 2p and (b) V 2p

attributed to sulfur with high oxidation state. While the diffraction peaks at 168.8 eV is mainly attributed to sulfur oxides, which are mainly caused by the oxidation of materials in the air. It can be seen from the XPS results that the V element is divided into two peaks in Fig. 8c, the diffraction peak at 516.8 eV of V $2p_{3/2}$ and the diffraction peak at 524.1 eV of V $2p_{1/2}$ are attributed to V^{2+}. Compared to the Ni-V hydroxide/NF, the V 2p spectrum of (V, Ru) -NiS_2/NF has a gentle shift in the path of high energy. It is proved that there is a strong electron interaction between V and Ni in sulfide. The Ru 3p region is also given in Fig. 8d. The diffraction peak at 461.7 eV belongs to Ru $3p_{1/2}$, while the diffraction peak at 484.1 eV belongs to Ru $3p_{1/2}$. Fig. 8e is mainly the C 1s+Ru 3d spectrum[40], which is mainly divided into five peaks. The diffraction peak at 280.3 eV is attributed to Ru $3d_{5/2}$, and the diffraction peak at 283.7 eV can be assigned to Ru $3d_{3/2}$. The diffraction peaks at 284.6, 285.4 and 287.1 eV correspond to C-C bond, C-O bond and C=O bond, respectively. Combining the XPS results with the element mapping, it can be demonstrated that the as-prepared samples contains Ni, S, Ru and V elements, and there is a strong electron flow in the sulfide.

To verify the effect of metal doping on electrocatalytic properties, (V, Ru) -NiS_2/NF was tested in 1 mol/L KOH solution with a three-electrode system at room temperature. For comparison, commercial Pt/C, Ni hydroxide/NF, Ni-V hydroxide/NF and V-NiS_2/NF were used as references. The linear sweep voltammetric (LSV) curves of commercial Pt/C, Ni hydroxide/NF, Ni-V hydroxide/NF, V-NiS_2/NF and (V, Ru)-NiS_2/NF are shown in Fig. 9a. As expected, the Ni hydroxide/NF shows the poorest HER electrocatalytic activity with an overpotential of 210 and 391 mV at 10 and 100 mA·cm^{-2}, respectively, due to its fewer active sites and poor electric structure. In contrast, the (V, Ru)-NiS_2/NF catalyst displays an outstanding HER activity with a lower overpotential of 183 mV at the current density of 100 mA·cm^{-2}, close to the electrocatalytic property of commercial Pt/C sample, exceeding that of Ni-V hydroxide/NF (344 mV) and V-NiS_2/NF (244 mV). The significantly improved electrocatalytic property of (V, Ru)-NiS_2/NF might be attributed to the successful sulfuration and

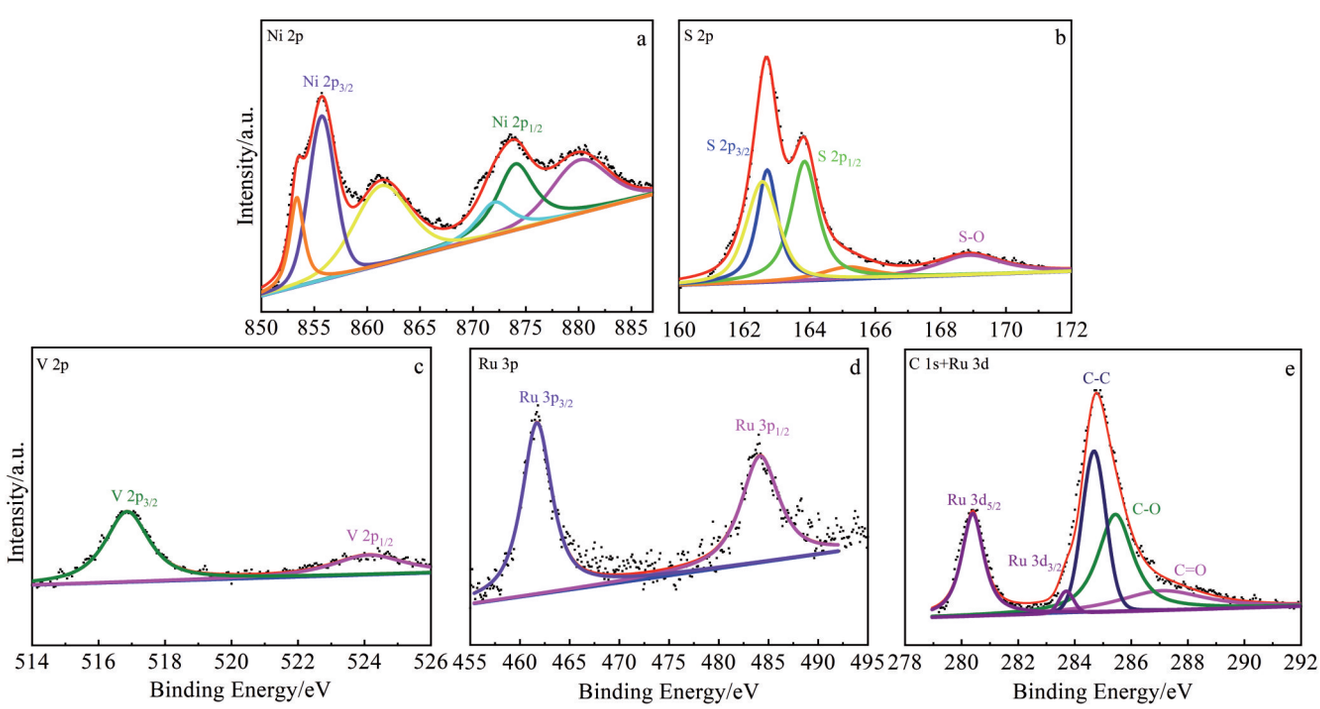

Fig.8 XPS spectra of (V, Ru)-NiS_2/NF: (a) Ni 2p, (b) S 2p, (c) V 2p, (d) Ru 3p, and (e) C 1s+Ru 3d

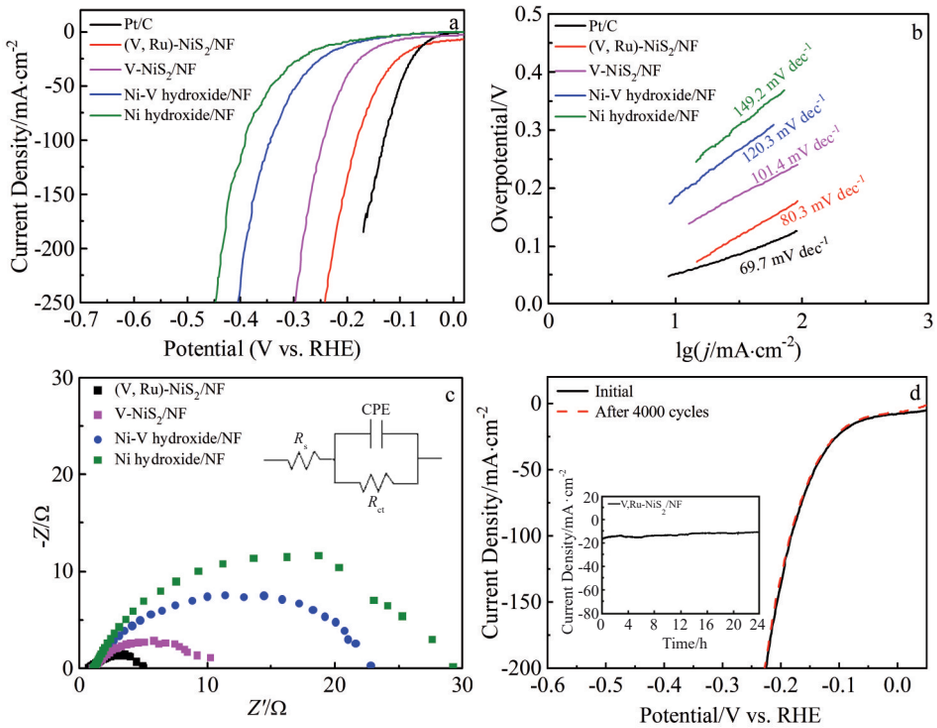

Fig.9 Electrochemical performances of Pt/C, Ni hydroxide/NF, Ni-V hydroxide/NF, V-NiS_2/NF, (V, Ru)-NiS_2/NF: (a) HER polarization curves, (b) Tafel plots, (c) Nyquist plots, and (d) time-dependent current density curve and LSV curve of (V, Ru)-NiS_2/NF before and after 4000 cycles (for all the measurements, *iR*-compensation is performed; the scan rate is 2 $mV·s^{-1}$ and electrolyte solution is 1 mol/L KOH)

the synergetic effect between V and Ru. The Tafel slopes in Fig.9b can clearly reflect the HER kinetics. The Tafel slope of (V, Ru)-NiS_2/NF is 80.3 $mV·dec^{-1}$, smaller than that of V-NiS_2/NF (101.4 $mV·dec^{-1}$), Ni-V hydroxide/NF (120.3 $mV·dec^{-1}$) and Ni hydroxide/NF (149.2 $mV·dec^{-1}$), indicating that (V, Ru)-NiS_2/NF has the highest intrinsic activity and the fastest hydrogen evolution rate in all samples except commercial Pt/C. Generally speaking, the hydrogen evolution process is mainly divided into two steps including Volmer reaction and Heyrovsky reaction[22,41]. According to the previous reports, as the limiting step of the hydrogen evolution reaction, the theoretical Tafel slopes of different steps are also different, for example, the theoretical Tafel slopes of Volmer reaction and Heyrovsky reaction are 120 and 40 $mV·dec^{-1}$, respectively, while the theoretical Tafel slopes of Tafel reaction is 30 $mV·dec^{-1}$. As shown in Fig.9b, the value of Tafel slope of (V, Ru)-NiS_2/NF is 80.3 $mV·dec^{-1}$, indicating that the rate-limiting step of (V, Ru)-NiS_2/NF is Volmer-Heyrovsky reaction in HER process. As far as we know, (V, Ru)-NiS_2/NF is the most prominent electrocatalyst reported in the literatures (Table 1). Moreover, the electrochemical impedance spectroscopy (EIS) can also intuitively reflect the electrocatalytic activities of the as-synthesized samples (Fig.9c). It can be seen that (V, Ru)-NiS_2/NF displays the smallest Nyquist semicircle compared with V-NiS_2/NF, Ni-V hydroxide/NF, and Ni hydroxide/NF, implying that (V, Ru)-NiS_2/NF has the lowest charge-transfer resistance and the fastest electron transfer rate during HER process[40–51]. Additionally, in order to objectively understand the electrocatalytic performance of the above catalyst, the electrochemical active surface areas (ECSAs) measurements were carried out by testing the double-layer capacitances (C_{dl}) of the samples at different scan rates. The C_{dl} value of (V, Ru)-NiS_2/NF is 54.3 $mF·cm^{-2}$, which is higher than that of V-NiS_2/NF (36.6 $mF·cm^{-2}$), Ni-V hydroxide/NF (3.1 $mF·cm^{-2}$), Ni hydroxide/NF (1.7 $mF·cm^{-2}$) in Fig. 10. Compared with other as-prepared samples, the (V, Ru)-NiS_2/NF has the largest electrochemical surface area. The stability of electrocatalyst is also an extremely vital factor to evaluate the HER activity. Fig. 9d exhibits that after 4000 cycles of CV cycles, the LSV curve of is akin to that of the initial cycle, Besides, the (V, Ru)-NiS_2/NF electrode can maintain the outstanding durability for 24 h at the current density of 18 $mA·cm^{-2}$. Above results prove that (V, Ru)-NiS_2/NF is a promising electrocatalyst both in terms of cost and electrochemical performance.

In addition to the stability of electrochemical performance, we also need to test the stability of the structure and its valence state. Therefore, the XRD, SEM and XPS measurements were carried out. As observed in Fig. 11, the XRD peak of the tested sample is similar to the initial peak and the position of diffraction peak has no shift. Furthermore, the tested samples still keep initial golf-like morphology after long-time durability test, proving that the structural stability of (V, Ru)-NiS_2/NF is excellent. Meanwhile, the XPS result of tested sample is shown in Fig. 12. The signal peaks of Ni 2p, S 2p, V 2p, Ru 3p and C 1s do not change, displaying that the (V, Ru)-NiS_2/NF catalyst has no chemical reaction during electrochemical testing. As displayed in Table 2, ICP measurement is used to detect the

Table 1 Comparison of HER activity in alkaline media between (V, Ru)-NiS_2/NF and recently reported HER electrocatalysts

Catalysts	Electrolytes	Overpotential@j/mV@mA·cm^{-2}	Tafel slope/mV·dec^{-1}	Ref.
(V, Ru)-NiS_2/NF	1 mol·L^{-1} KOH	38@10 183@100	80.3	This work
NiS_2/GS	1 mol·L^{-1} KOH	190@10 314@100	85	[47]
NiS_2 HMS	1 mol·L^{-1} KOH	219@10	157	[48]
V-MoS_2-Ni_xS_y/NF	1 mol·L^{-1} KOH	68@10 155@100	80.4	[39]
P-Ni_3S_2-NiS/NF	1 mol·L^{-1} KOH	141@10 290@50	75	[49]
Fe,C-MoS_2/Ni_3S_2-450	1 mol·L^{-1} KOH	188@10	95	[50]
$Ni_{0.85}Se$/Ni_3S_2/NF-1.5	1 mol·L^{-1} KOH	145@10	130	[51]
Mo-doped Ni_3S_2-3	1 mol·L^{-1} KOH	170@10 279@50	112	[52]
Graphene-NiS-NiS_2-Ni_3S_4	1 mol·L^{-1} KOH	68@10	79	[53]

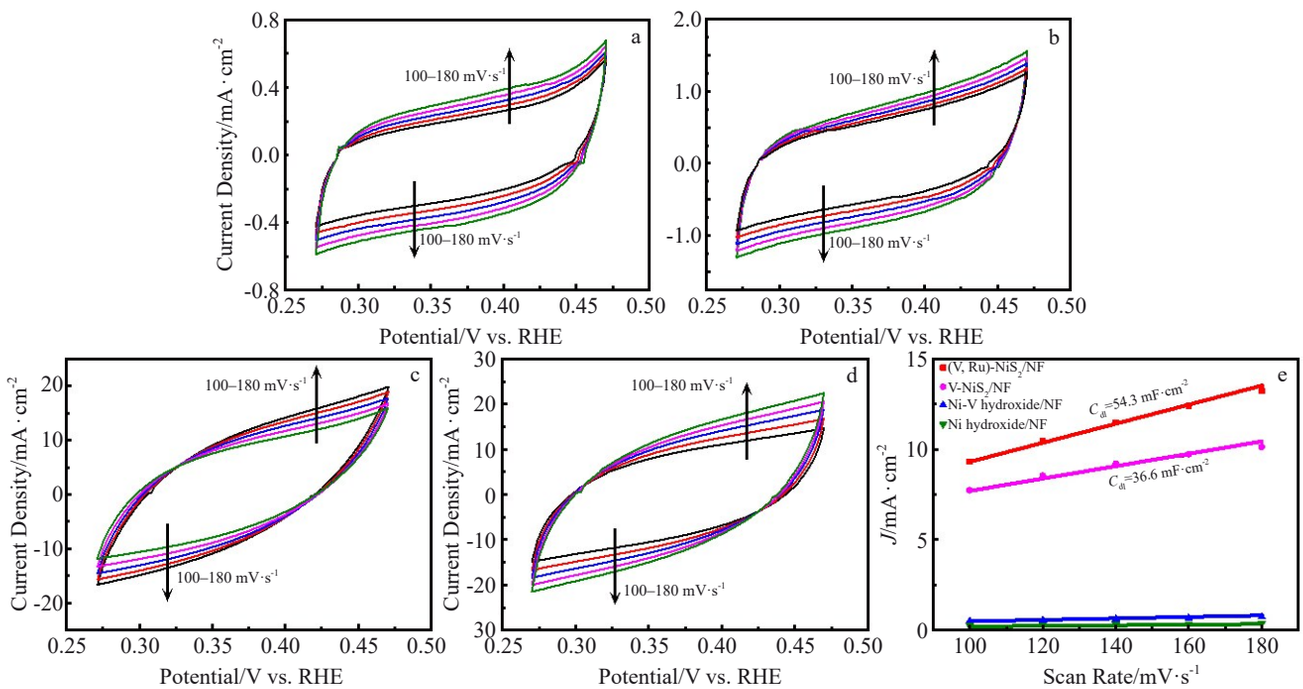

Fig.10 Cyclic voltammetry curves of Ni hydroxide/NF (a), Ni-V hydroxide/NF (b), V-NiS_2/NF (c) and (V, Ru)-NiS_2/NF (d) in 1 mol/L KOH at different scan rates; (e) C_{dl} values of all the samples

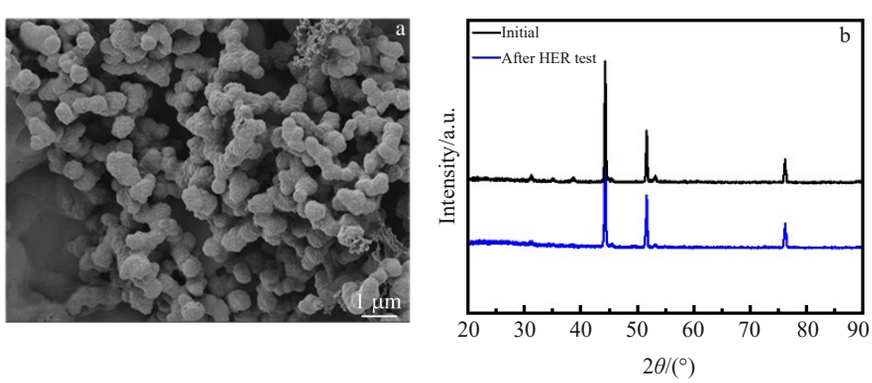

Fig.11 SEM image (a) and XRD patterns (b) of (V, Ru)-NiS_2/NF after HER durability test

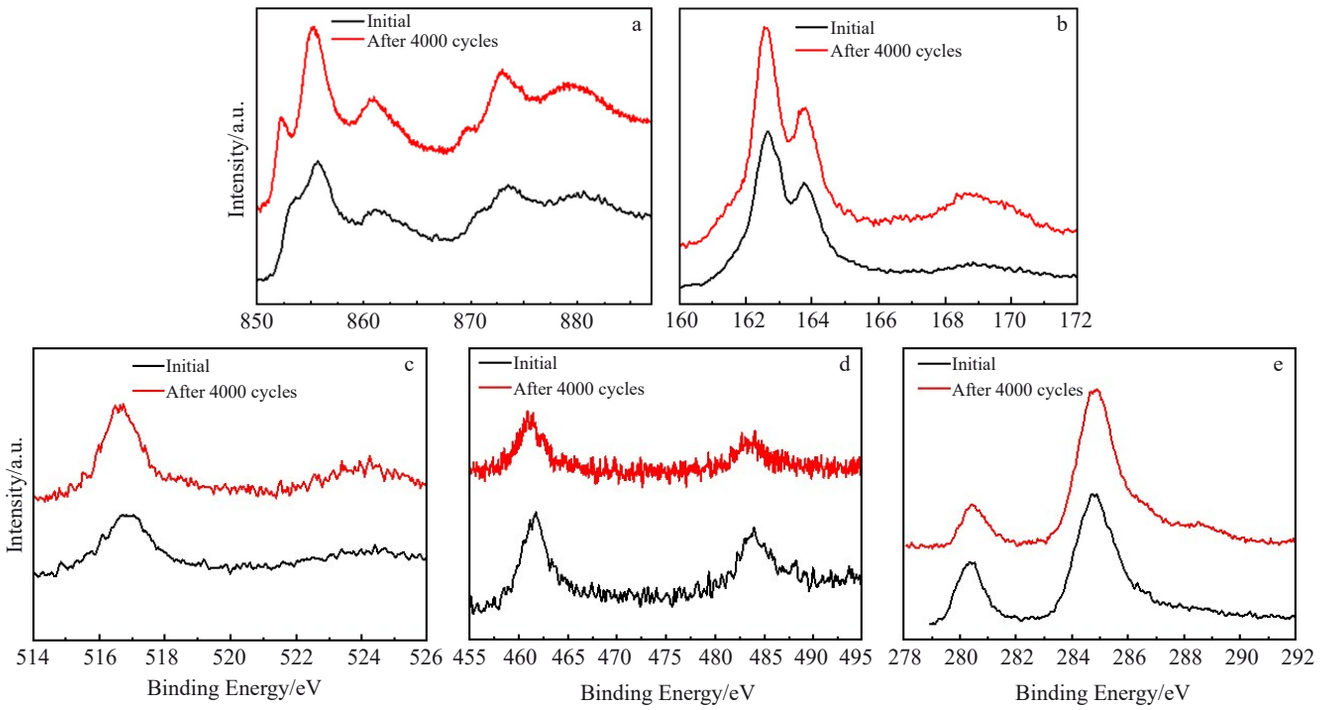

Fig.12 XPS spectra of (V, Ru)-NiS_2/NF after HER: (a) Ni 2p, (b) S 2p, (c) V 2p, (d) Ru 3p, and (e) C 1s+Ru 3d

Table 2 ICP results of (V, Ru)-NiS_2/NF before and after reaction (wt%)

Element	Before reaction	After reaction
Ni	48.05	46.73
V	17.63	17.12
Ru	5.99	5.06

metal content before and after reaction[52–53]. The ICP results indicate that before electrochemical testing, the atomic ratio of Ni, V and Ru of (V, Ru) -NiS_2/NF is 48.05%, 17.63%, and 5.99%, respectively, and after 24 h of electrochemical testing, the atomic ratio of Ni, V and Ru of (V, Ru) -NiS_2/NF is 46.73%, 17.12%, and 5.06%, respectively, demonstrating that after a long period of electrochemical testing, the dissolved amount of metal element is almost negligible and the high durability of (V, Ru)-NiS_2/NF catalyst is further certified.

3 Conclusions

1) A cost-effective and simple method is designed and developed to obtain golf-like (V, Ru) -NiS_2 microspheres coated on Ni foam via solvothermal method and vulcanization method at low temperature. The obtained (V, Ru) -NiS_2/NF composite can stably maintain spherical morphology in long time stability testing. Furthermore, vanadium and ruthenium co-doping can not only optimize the electronic structure and accelerate the electron transfer, but also have a synergistic effect on reducing the Gibbs free energy of the reaction as extra active sites, thus speeding up the reaction process and improving the reaction efficiency.

2) The (V, Ru)-NiS_2/NF electrocatalyst exhibits competitive electrochemical performance in alkaline solution with a low overpotential of 38 mV at 10 mA·cm^{-2}, and a Tafel slope of 80.3 mV·dec^{-1}. In addition, it has excellent stability in electrochemical performance and morphology structure.

References

1 Zheng Y, Jiao Y, Jaroniec M *et al*. *Angewandte Chemie International Edition*[J], 2015, 54(1): 52
2 Safizadeh F, Ghali E, Houlachi G. *International Journal of Hydrogen Energy*[J], 2015, 40(1): 256
3 Strmcnik D, Lopes P P, Genorio B *et al*. *Nano Energy*[J], 2016, 29: 29
4 Voiry D, Yang J, Chhowalla M. *Advanced Materials*[J], 2016, 28(29): 6197
5 Jin H, Liu X, Chen S *et al*. *ACS Energy Letters*[J], 2019, 4(4): 805
6 Guo S, Li X, Li J *et al*. *Nature Communications*[J], 2021, 12(1): 1
7 Chen Y, Ji S, Sun W *et al*. *Angewandte Chemie*[J], 2020, 132(3): 1311
8 Kataoka Y, Sato K, Miyazaki Y *et al*. *Energy & Environmental Science*[J], 2009, 2(4): 397
9 Xie J, Zhang H, Li S *et al*. *Advanced Materials*[J], 2013, 25(40): 5807
10 Lu Q, Yu Y, Ma Q *et al*. *Advanced Materials*[J], 2016, 28(10): 1917
11 Li J, Hu J, Zhang M *et al*. *Nature Communications*[J], 2021, 12(1): 1
12 Holladay J D, Hu J, King D L *et al*. *Catalysis Today*[J], 2009, 139(4): 244
13 Zhou K L, Wang Z, Han C B *et al*. *Nature Communications*[J], 2021, 12(1): 1
14 Li Z, Yao Y, Niu Y *et al*. *Chemical Engineering Journal*[J],

2021, 418: 129 321
15 Liu Y, Dou Y, Li S *et al*. *Small Methods*[J], 2021, 5(2): 2 000 701
16 Yang M, Jiao L, Dong H *et al*. *Science Bulletin*[J], 2021, 66(3): 257
17 Zhang R L, Duan J J, Feng J J *et al*. *Journal of Colloid and Interface Science*[J], 2021, 587: 141
18 Wang J, Zeng H C. *ACS Applied Materials & Interfaces*[J], 2019, 11(26): 23 180
19 Lu Q, Yu Y, Ma Q *et al*. *Advanced Materials*[J], 2016, 28(10): 1917
20 Kochat V, Apte A, Hachtel J A. *Advanced Materials*[J], 2017, 29(43): 1 703 754
21 Anantharaj S, Aravindan V. *Advanced Energy Materials*[J], 2020, 10(1): 1 902 666
22 Zhong W, Xiao B, Lin Z *et al*. *Advanced Materials*[J], 2021, 33(9): 2 007 894
23 Yin J, Jin J, Zhang H *et al*. *Angewandte Chemie*[J], 2019, 131(51): 18 849
24 Liang Y, Yang Y, Xu K *et al*. *Journal of Catalysis*[J], 2020, 381: 63
25 Yan J, Wu H, Chen H *et al*. *Journal of Materials Chemistry A*[J], 2017, 5(21): 10 173
26 Kuang P, He M, Zhu B *et al*. *Journal of Catalysis*[J], 2019, 375: 8
27 Li Q, Wang D, Han C *et al*. *Journal of Materials Chemistry A*[J], 2018, 6(18): 8233
28 Kuang P, He M, Zou H *et al*. *Applied Catalysis B: Environmental*[J], 2019, 254: 15
29 Wang H, Wang Y, Zhang J *et al*. *Nano Energy*[J], 2021, 84: 105 943
30 Mao X, Liu Y, Chen Z *et al*. *Chemical Engineering Journal*[J], 2022, 427: 130 742
31 Hu Z, Zhang L, Huang J *et al*. *Nanoscale*[J], 2021, 13(17): 8264
32 He J, Liu F, Chen Y *et al*. *Chemical Engineering Journal*[J], 2022, 432: 134 331
33 Wang W, Zhao H, Du Y *et al*. *Chemistry – A European Journal*[J], 2021, 27(7): 2463
34 Yan J, Wu H, Chen H *et al*. *Journal of Materials Chemistry A*[J], 2017, 5(21): 10 173
35 Guan Y, Feng Y, Wan J *et al*. *Small*[J], 2018, 14(27): 1 800 697
36 Chang Q, Ma J, Zhu Y *et al*. *ACS Sustainable Chemistry & Engineering*[J], 2018, 6(5): 6388
37 Yu J, Guo Y, She S *et al*. *Advanced Materials*[J], 2018, 30(39): 1 800 047
38 Pu Z, Amiinu I S, Kou Z *et al*. *Angewandte Chemie International Edition*[J], 2017, 56(38): 11 559
39 Wang W, Zhao H, Du Y *et al*. *Sustainable Energy & Fuels*[J], 2021, 5(3): 698
40 Zhou F, Sa R, Zhang X *et al*. *Applied Catalysis B: Environmental*[J], 2020, 274: 119 092
41 Wang W, Zhao H, Du Y *et al*. *Applied Surface Science*[J], 2020, 534: 147 626
42 Wu X, Yang B, Li Z *et al*. *RSC Advances*[J], 2015, 5(42): 32 976
43 Tian T, Huang L, Ai L *et al*. *Journal of Materials Chemistry A*[J], 2017, 5(39): 20 985
44 Zhou B, Li J, Zhang X *et al*. *Journal of Alloys and Compounds*[J], 2021, 862: 158 391
45 Lv X, Liu G, Liu S *et al*. *Crystals*[J], 2021, 11(4): 340
46 Ding Z, Wang K, Mai Z *et al*. *International Journal of Hydrogen Energy*[J], 2019, 44(45): 24 680
47 Li J, Yang Z, Lin Y *et al*. *New Journal of Chemistry*[J], 2020, 44(20): 8578
48 Wang H, Zhang W, Zhang X *et al*. *Nano Research*[J], 2021, 14: 4857
49 Zhang Y, Zhou H, Wang H *et al*. *Chemical Engineering Journal*[J], 2021, 418: 129 343
50 Zhang Y, Hu L, Zhou H *et al*. *ACS Applied Nano Materials*[J], 2022, 51: 391
51 Zhang Y, Hu L, Zhang Y *et al*. *Applied Catalysis B: Environmental*[J], 2022, 315: 121 540
52 Chang J, Li K, Wu Z *et al*. *ACS Applied Materials & Interfaces*[J], 2018, 10(31): 26 303
53 Huang W H, Li X M, Yu D Y *et al*. *Nanoscale*[J], 2020, 12(38): 19 804

V，Ru共掺杂NiS_2高尔夫微球作为碱性介质析氢反应的高效电催化剂

王文思[1]，刘　辉[1]，余泽锦[1]，卢　军[3]，冯　丰[1]，桓源峰[1]，赵云昆[1]，余建民[3]，卿　山[2]，毕向光[1,2]

(1. 昆明贵研催化剂有限责任公司，云南 昆明 650106)

(2. 昆明理工大学 冶金与能源工程学院，云南 昆明 650106)

(3. 昆明贵金属研究所，云南 昆明 650106)

摘　要：通过溶剂热法和滴钌法（室温）将钒和钌引入到NiS_2中，并制备了包覆在泡沫镍上的V，Ru共掺杂NiS_2微球(V, Ru)-NiS_2/NF电催化剂。通过硫化过程产生粗糙的高尔夫球状结构暴露出丰富的活性位点，此外，钒和钌的协同作用可以优化NiS_2的电子结构，提供额外的催化活性位点，进一步增强本征催化活性。泡沫镍的加入对催化材料起到支撑作用，避免聚集，同时提高导电性。结果表明，(V, Ru)-NiS_2/NF电催化剂在碱性条件下表现出优异的电催化性能和优异的析氢反应稳定性。在10 mA·cm^{-2}的电流密度下，(V, Ru)-NiS_2/NF提供了38 mV的过电位，小于商业Pt/C的过电位，并且具有较低的Tafel斜率（80.3 mV·dec^{-1}）、较高的电化学活性表面（ECSA）和在KOH溶液中24 h出色的稳定性。

关键词：钒；钌；掺杂；析氢反应

作者简介：王文思，男，1995年生，硕士，工程师，昆明贵研催化剂有限责任公司，云南 昆明 650106，E-mail：wws372295@163.com